Mars Science Laboratory Rover Mobility Bushing Development

Benjamin Riggs*

Abstract

NASA's Mars Science Laboratory (MSL) Project will send a six-wheeled rover to Mars in 2009. The rover will carry a scientific payload designed to search for organic molecules on the Martian surface during its primary mission. This paper describes the development and testing of a bonded film lubricated bushing system to be used in the mobility system of the rover.

Introduction

The MSL Rover Mobility System contains several pivots that are tightly constrained with respect to mass and volume. These pivots are also exposed to relatively low temperatures (-135°C) during operation. The combination of these constraints led the mobility team to consider the use of solid film lubricated metallic bushings and dry running polymeric bushings in several flight pivot applications.

A test program was developed to mitigate the risk associated with using these materials in critical pivots on the MSL vehicle. The program was designed to characterize bushing friction and wear performance over the expected operational temperature range (-135°C to +70°C). Seven different bushing material / lubricant combinations were evaluated to aid in the selection of the final flight pivot bushing material / lubricant combination.

Background

The mobility team recognized during the rover preliminary design phase that the large size and mass of the new vehicle required a fresh look at the design approach for many of its pivots. The rover required pivots that could tolerate intermittent, low speed (<2.5 rpm) dithering motion at operational temperatures that precluded the use of wet lubricants. After an extensive trade study that assessed mass, complexity and volumetric efficiency the team decided to pursue main pivots based on primarily on flanged bushings. Flanged bushings provided a simple, robust, mass-effective solution to the design challenges associated with the highly loaded main mobility pivots.

With the general design approach selected the team accelerated its search for viable material/lubrication options for the bushings. A large number of material and lubrication options were considered for use in the pivots including various bronze bushing alloys, zinc aluminum, polymeric materials, and coated stainless steel. Although a number of these materials had merit the team selected coated, gall-resistant stainless steel bushings for the initial test series on the basis of compressive strength, gall resistance in the event of lubricant failure and published coated coefficient of friction information. Isolating a bushing material also allowed for a manageable set of bushing material, mating surface and lubricant combinations during testing. Three candidate bonded film lubricants with inorganic binders were selected to coat the stainless steel bushings during the initial test series.

Testing

The unproven combination of bonded film lubricants and bushing materials in the rover mobility pivots required testing to enable their use on the flight vehicle. Friction and wear performance data was also desired to enable more accurate modeling of the pivots in dynamic simulations. These factors led the design team to plan a multiphase test series to select a final bonded film lubricant and characterize the friction and wear performance of the bushings over the pivot operational temperature range.

* Jet Propulsion Laboratory/California Institute of Technology, Pasadena, CA

Phase One: Initial Ring on Cylinder Testing

Since the second phase of the test series involved a relatively complex, flight-like pivot and test apparatus there was a desire to "start simple" and get some initial data on the candidate bonded film / bushing systems before resources were committed to the more elaborate, follow-on setup. Due to looming review dates and a desire to get the initial test series completed quickly the team investigated various bushing test resources at other facilities. Fortunately a preexisting developmental bushing test setup at NASA/Glenn Research Center (GRC) was located that could be slightly modified to complete the desired initial testing of the bushing / lubricant systems. The GRC team quickly reconfigured their setup and test samples were fabricated so that testing could begin.

The testing consisted of loading PTFE infused hard anodized 7075 rings & PTFE infused Ti6Al4V rings against various bonded film coated stainless steel shafts to produce a projected bearing stress of approximately 6895 kPa (1000 psi). The test fixture rotated the coated shaft against the ring in a constant dithering motion of ±2 degrees. Testing was performed in lab air at 40% relative humidity for the first 69 cycles then in a CO_2 purged glove box for the remainder of the 4200 total cycles (all at 23°C). Friction torque was measured throughout the test so that coefficient of friction values could be calculated at the completion of testing. Three samples of each material combination were tested during the series. The summarized results of the GRC test series are listed in Table 1 [1].

Table 1: Phase One Bushing Test Results

Ring Material	Shaft Material / Coating	Mean Coefficient of Friction for 3 Tests
Al 7075-T7351 with PTFE hard anodized coating	Stainless steel coated with MoS_2 based bonded film lubricant with "phosphate-like" binder	0.084 std dev 0.028
Al 7075-T7351 with PTFE hard anodized coating	Stainless steel coated with PTFE based bonded film lubricant with "phosphate-like" binder	0.120 std dev 0.020
Al 7075-T7351 with PTFE hard anodized coating	Stainless steel coated with MoS_2 based bonded film lubricant with silicate binder	0.139 std dev 0.054
Ti6Al4V with PTFE anodic coating	Stainless steel coated with MoS_2 based bonded film lubricant with "phosphate-like" binder	0.070 std dev 0.031
Ti6Al4V with PTFE anodic coating	Stainless steel coated with PTFE based bonded film lubricant with "phosphate-like" binder	0.194 std dev 0.047
Ti6Al4V with PTFE anodic coating	Stainless steel coated with MoS_2 based bonded film lubricant with silicate binder	0.145 std dev 0.005
Al 7075-T7351 with PTFE hard anodized coating	Bare stainless steel	0.266 std dev 0.070
Ti6Al4V with PTFE anodic coating	Bare stainless steel	0.212 std dev 0.048

Phase Two: Application Specific Bushing Testing

Phase Two of the Bushing Test Series was designed to characterize bushing friction and wear behavior in a flight-like pivot assembly over the expected mobility operational temperature range (-135°C to +70°C). Several different bushing materials and coatings were tested during this test series to allow the team to select the best combination for the flight mobility pivots based on data from a representative pivot.

Test Setup

The bushing test hardware was designed to mimic a portion of the MSL Rover's Main Differential Pivot (MDP). The flight pivot assembly is comprised of two flanged bushings located between a central pivot shaft and a hollow cylindrical housing (Figure 2). In the test assembly (Figures 1 & 3) the central pivot shaft was attached to a fixture comprised of an aluminum block, several C-channel sections and a baseplate. The cylindrical housing was attached to a driveshaft driven by a motion controlled DC servomotor through several flexible shaft couplings and a torquemeter. This torquemeter was used to measure the friction torque generated in the pivot assembly during testing.

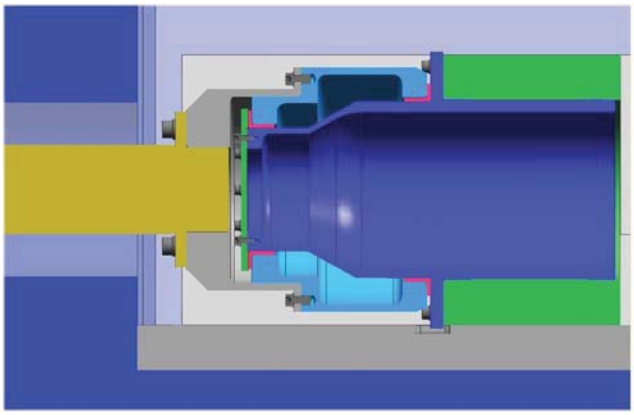

Figure 1: Test Assembly

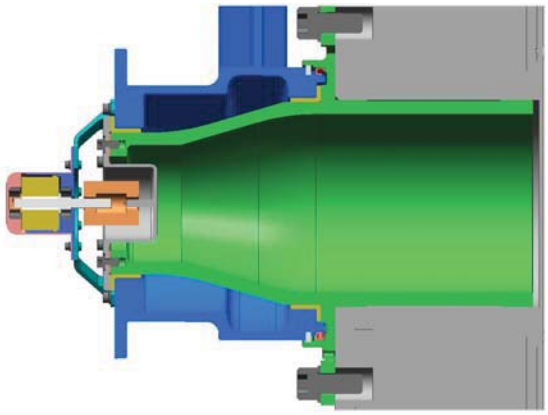

Figure 2: Flight MDP Assembly

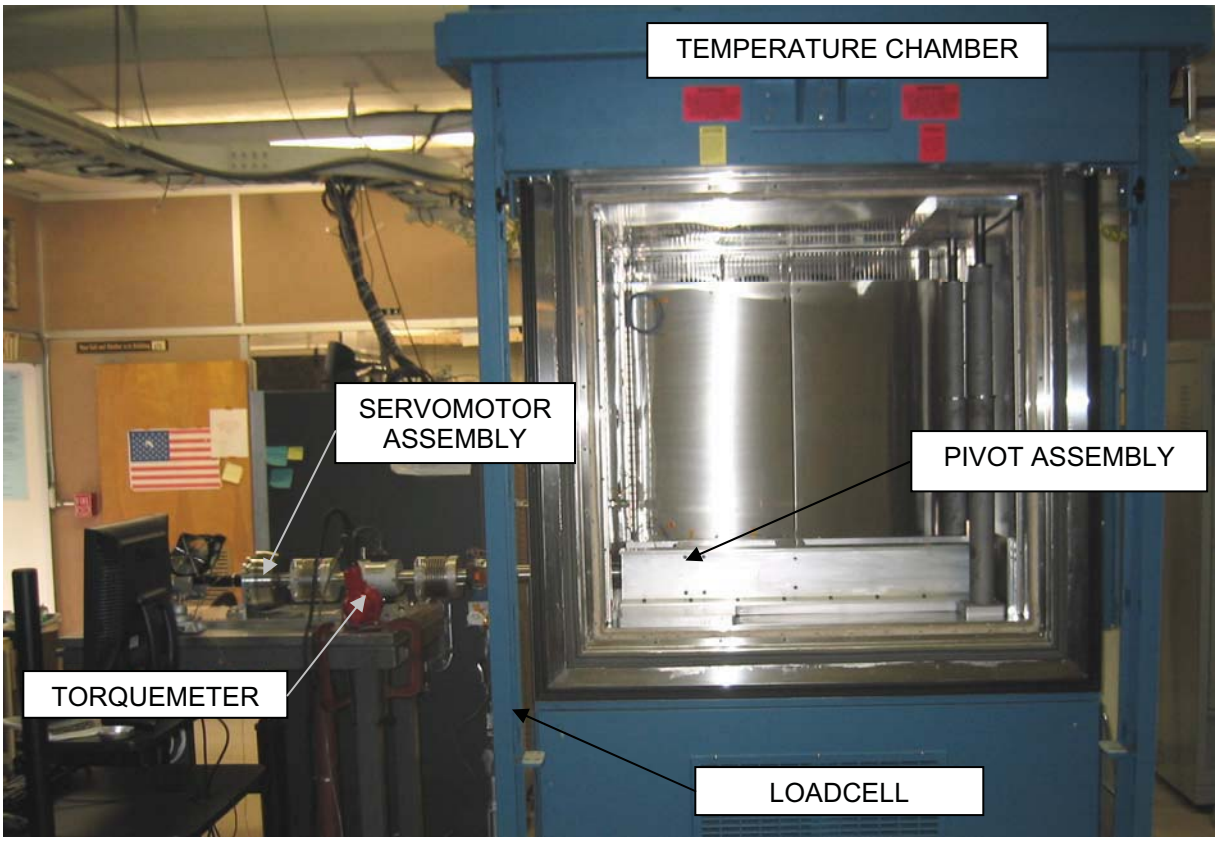

Figure 3: Bushing Test Hardware in Temperature Chamber

A pillow block assembly, turnbuckle, and grounded load cell string were attached to the driveshaft to apply a known moment on the pivot assembly during testing. This known moment produced reaction loads on the bushings roughly equivalent to those expected during vehicle traverse on Mars.

The DC servomotor rotated the driveshaft and cylindrical housing through a specific dithering angular motion profile during bushing testing. This motion profile was developed to replicate the oscillating motion of the Flight Main Differential Pivot.

The pivot assembly, comprised of the bushing pair, central pivot shaft and cylindrical housing, was mounted inside a temperature chamber that was used to drive the assembly through a specific temperature profile. The chamber also provided a humidity-controlled, dry nitrogen environment throughout testing. During test planning the option of testing in a CO_2 environment was discussed. Although the CO_2 environment would have been preferred as the Martian atmosphere is predominantly CO_2, the cost and schedule impact associated with that testing was prohibitive. The team also felt that testing in dry Nitrogen would yield acceptable results based on test data from the Phase One Testing at GRC.

Bushing Material / Lubrication Description

Seven different bushing material / bushing lubricant combinations were evaluated as part of the test series. Two MoS_2-based bonded film lubricants were selected for the test series, a bonded film with a "phosphate-like" binder and a bonded film with a silicate binder. These lubricants were coupled a stainless steel alloy based on its anti-galling characteristics in the event of coating failure. Polyamide-imide and polyimide samples were added to the test series after initial testing of the first bonded film sample revealed less than ideal bushing wear behavior. These two polymeric bushing materials were selected based on their suitability for the low temperature, dry running flight pivot environments.

All bushing samples were run against either 7075-T7351 Aluminum or Ti6Al4V shafts and housings that matched potential flight pivot materials. The aluminum shafts and housings were coated with a PTFE infused hard anodized coating. All titanium parts were coated with a PTFE infused anodic coating. Both of these coatings were applied to provide a hard, low friction, wear resistant bearing surface. Table 2 summarizes the bushing material and lubricants used for each test in the series:

Table 2: Phase Two Testing Material Matrix

Test Date	Housing & Shaft Material	Bushing Material	Bushing Coating
6/29/06	Al 7075-T7351 with PTFE infused hard anodized coating	Stainless steel	MoS_2 based bonded film lubricant with silicate binder
9/18/06	Al 7075-T7351 with PTFE infused hard anodized coating	Stainless steel	MoS_2 based bonded film lubricant with "phosphate-like" binder
9/25/06	Al 7075-T7351 with PTFE infused hard anodized coating	Polyamide-imide	None
10/24/06	Al 7075-T7351 with PTFE infused hard anodized coating	Polyimide	None
12/12/06	Al 7075-T7351 with PTFE infused hard anodized coating	Polyamide-imide	Braycote 601 Greaseplate
1/29/07	Ti6Al4V with PTFE infused anodic coating	Stainless steel	MoS_2 based bonded film lubricant with "phosphate-like" binder
2/7/07	Al 7075-T7351 with PTFE infused hard anodized coating	Stainless steel	None

Test Temperature / Cycling Profile

The bushing test temperature profile was generated to provide friction torque data throughout the expected pivot operational temperature range with an emphasis on the low side of range. The low temperature bias was selected as overall bushing clearance variances were most extreme at the low end of the temperature range. Also, low temperature friction and wear data for the bonded films and polymeric materials tested was very limited. The bushing test temperature profile and bushing test temperature/dither summary are listed in Table 3.

Table 3: Phase Two Bushing Testing Dither Cycle / Temperature Profile

Number of Dither Cycles	Temperature	Comments
10	+23°C	Initial check out, chamber door open
200	+23°C	Chamber door closed, N2 purge on
30	+47°C	
30	+70°C	
30	+47°C	
30	+23°C	
30	-9°C	
30	-43°C	
30	-73°C	
30	-105°C	
20	-120°C	Cycles added to prevent ice formation on feedthru
10	-130°C	Cycles added to prevent ice formation on feedthru
4720	-135°C	
30	-105°C	
30	-73°C	
30	-41°C	
30	-9°C	
200	+23°C	

Dither Cycling Profile

The dithering motion profile run during the bushing testing was formulated based on the output of Matlab code written by Jaime Waydo [2]. Her *Dither Analysis Code* calculated the main pivot (differential) dither angles produced by rock encounters during a simulated 60-kilometer vehicle traverse in a 20% rock field. The code output dither angle amplitude events for the 60-km traverse as shown in Table 4.

Table 4: Dither Event Count for 60 km Vehicle Traverse in 20% Rock Field

Main Pivot Dither Angle (θ) Range	Number of events for 60 km traverse	% of Total
θ < 5 degrees	3252	78%
5 degrees < θ < 15 degrees	450	11%
15 deg < θ < 20+ degrees	439	11%

Based on this output a simplified test dither cycle profile was formulated. The profile was based on three distinct dither amplitude cycles, a small angle cycle (±2 degrees), a medium angle cycle (±10 degrees) and a large angle cycle (±20 degrees). When these groupings were mapped to the frequencies generated by the Matlab code the following profile was developed. A 10-cycle set started with a ±20-

degree dither cycle followed by four ±2-degrees dither cycles, one ±10-degree dither cycle, and finally four more ±2-degrees dither cycles. The final test dither cycle profile is plotted in Figure 4

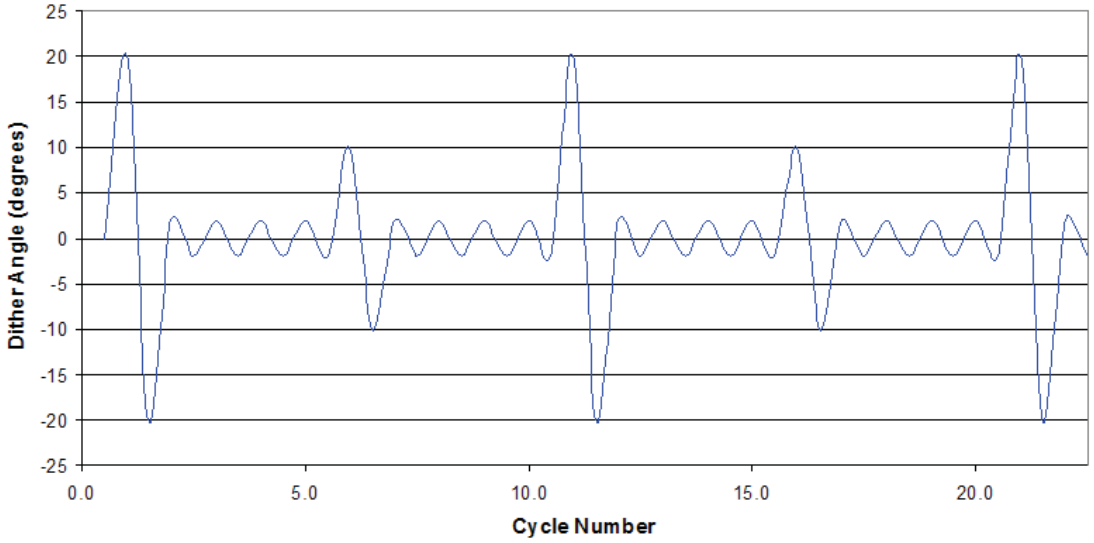

Figure 4: Bushing Test Dither Cycling Profile

This dither cycle profile was repeated until the total number of cycles planned at each temperature target was reached and the drive assembly was paused. The total number of dither cycles run for each test was based on a 60 kilometer total scaled to 80 kilometers (or four times the current 20-km mission traverse distance requirement). This scaling yielded a total bushing test dither cycle number of 5520 (for a 4x test).

The maximum angular rate of the servomotor output was set to 2.5 RPM for the duration of the dither testing. This angular rate was selected based on a combination of actuator/torque capabilities and expected maximum differential articulation rates during traverse.

Bushing Loading

The radial loads placed on the test bushings were intended to replicate a subset of those imparted on the flight MDP bushings during the primary mission of the vehicle. Dynamic loading of the bushings due to the touchdown or multi-wheel drops during traverse was not factored into the load calculations for the test bushings. Only the six wheels flat, 1G, 30 deg vehicle roll Adams model output values scaled to 3/8g equivalent loading were used to determine the target loading for bushing testing. The flight bushing radial loads and test loads are listed in Table 5. Also listed is the average bearing stress on the bushings due to radial loading and approximate contact stress values based on formulas from Roark's Formulas for Stress and Strain [3].

Table 5: Bushing Loading Summary

Bushing Location	Radial Bushing Load (N)	Average Bearing Stress (kPa)	Contact Stress (kPa)
MDP Inboard Bushing	5383	3.6 (0.520 ksi)	14.5 (2.1 ksi)
Test Inboard Bushing	6427	4.3 (0.622 ksi)	15.9 (2.3 ksi)
MDP Outboard Bushing	5127	4.9 (0.708 ksi)	17.9 (2.6 ksi)
Test Outboard Bushing	5267	5.0 (0.727 ksi)	18.6 (2.7 ksi)

The loading method employed in the bushing test setup did not allow the applied radial load to be matched for both the inboard and outboard bushing. As such the loading in the inboard test bushing was slightly higher than the target flight MDP inboard bushing radial load.

Although the moment-carrying load path for the flanged bushing pair was assumed to be purely radial for the loading calculations listed in Table 5, actual bushing loading in the test assembly proved that this assumption was at least partly flawed. The most significant bushing wear in the initial tests was on the edge of the thrust face of the bushing indicating that at least part of the moment applied to the test setup was being reacted out on the thrust faces of the bushings. This result was not altogether unexpected as the test pivot assembly geometry does have a redundant moment carrying capability through the thrust faces of the bushings. The radial gaps in the pivot required due to dissimilar coefficient of thermal expansion values between the gall resistant stainless steel bushing material and the pivot structure allowed this redundant load path to be possible. Although the loading produced in test setup is still thought to be representative of the flight environment, exact contact stress value determination for the bushings was significantly complicated by this non-ideal loading. If this tribological combination is selected for future designs careful thought should be employed to produce at design with a more tightly constrained load path.

Results

Friction Torque

The friction torque measurements obtained during the bushing test series are plotted in Figures 5 through 11. Housing temperature (shown in red) during the measurements was also plotted on a secondary axis for reference. Each plot was generated with the same scale on the X and Y axes to permit a quick visual comparison of the friction torque profile for each test.

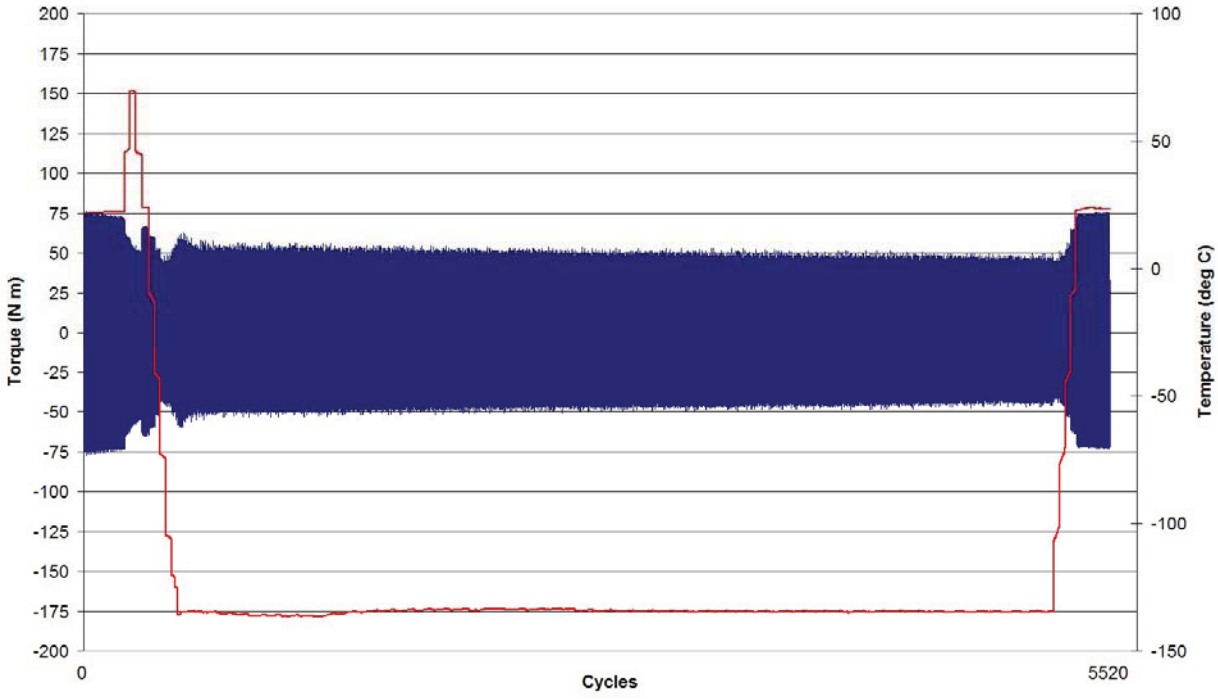

Figure 5: Friction Torque Plot
"Phosphate-like" Binder MoS_2 Bonded Film Coated Bushings vs. Anodized Aluminum)

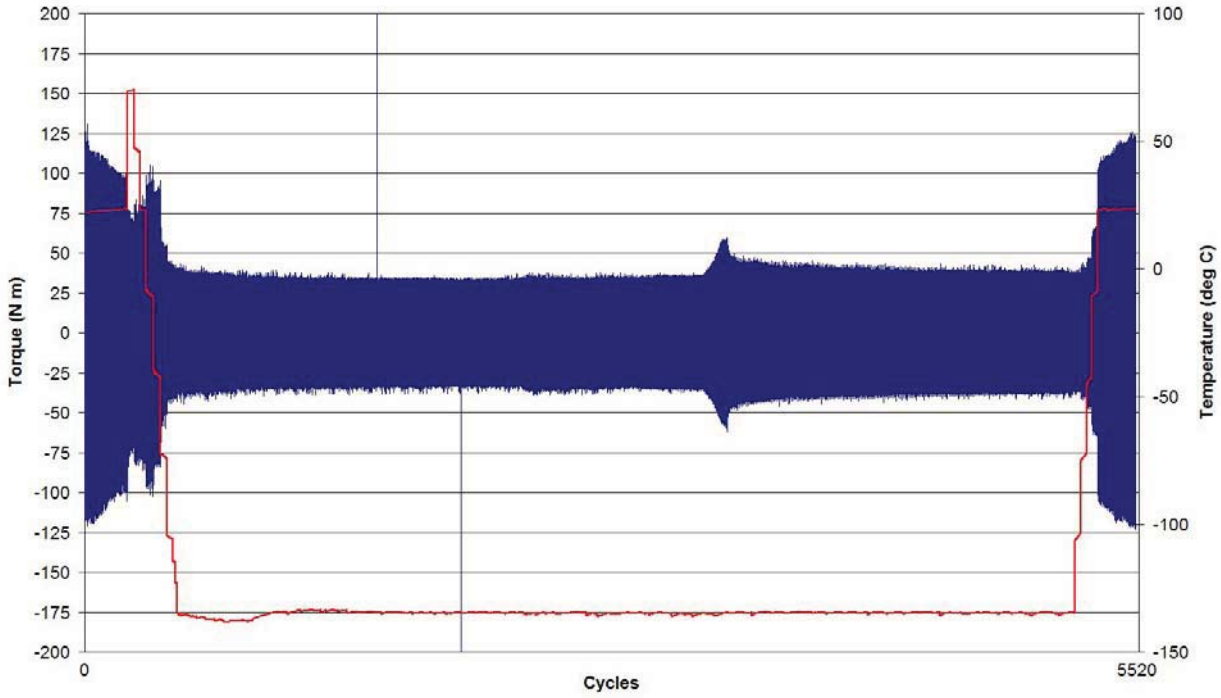

Figure 6: Friction Torque Plot
Silicate Binder MoS_2 Bonded Film Coated Bushings vs. Anodized Aluminum)

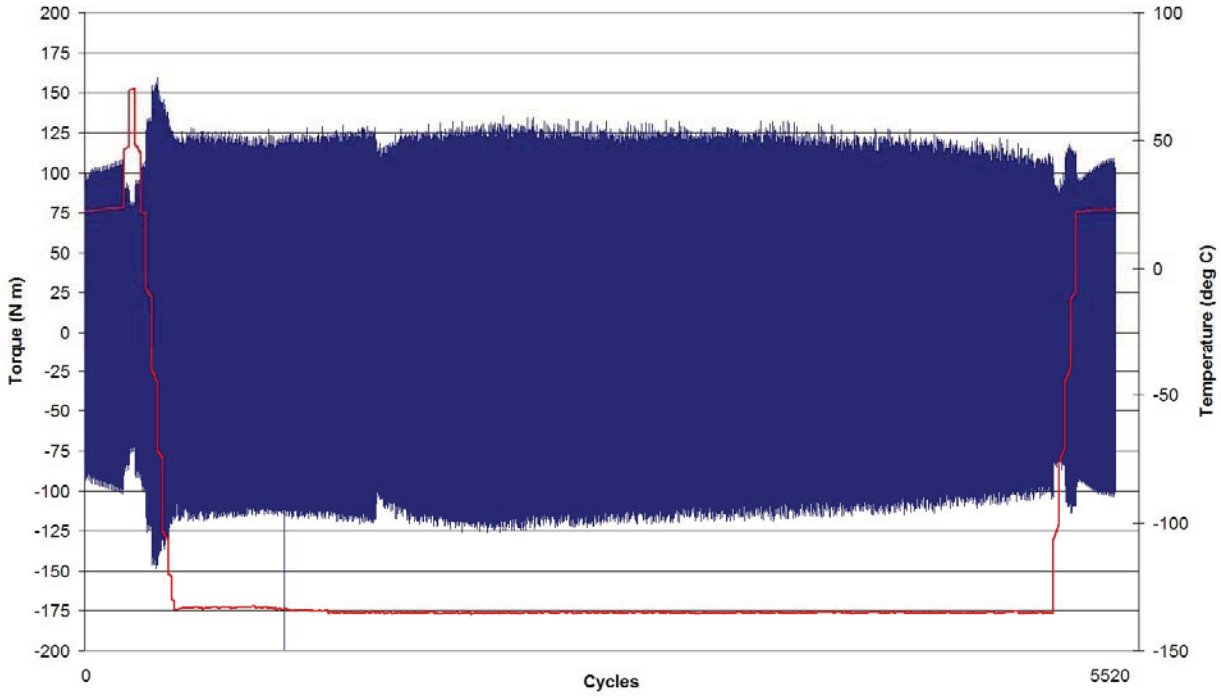

Figure 7: Friction Torque Plot
Polyamide-imide Bushings vs. Anodized Aluminum

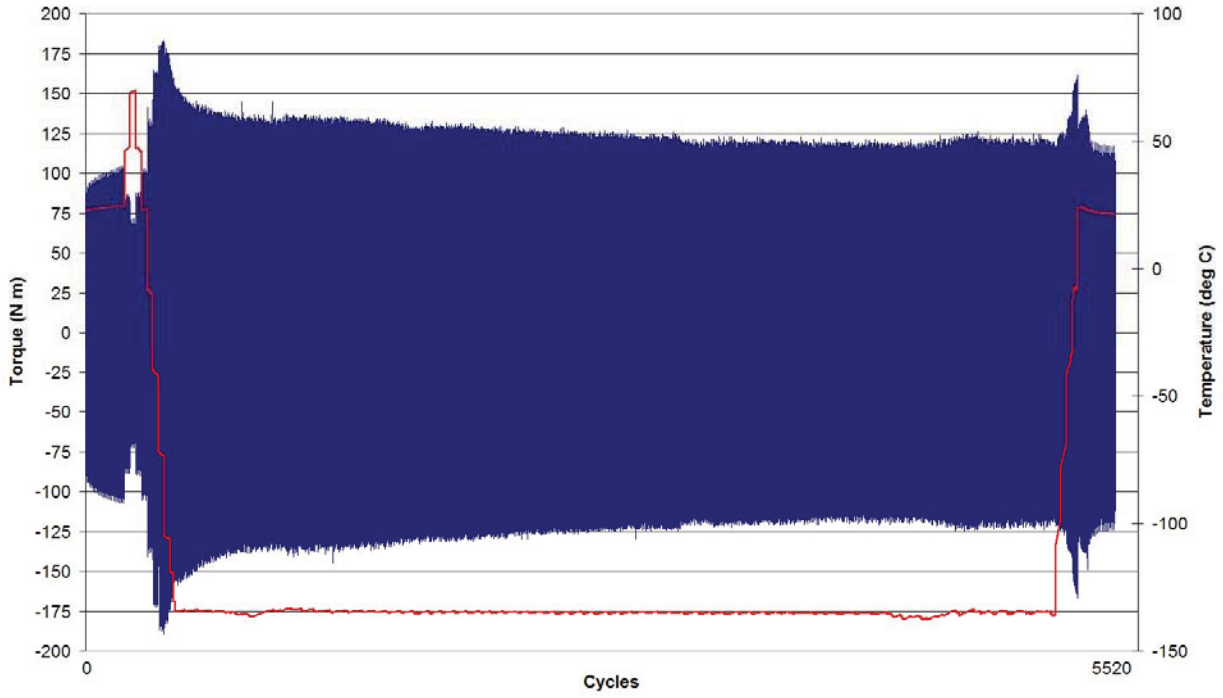

Figure 8: Friction Torque Plot
Polyimide Bushings vs. Anodized Aluminum

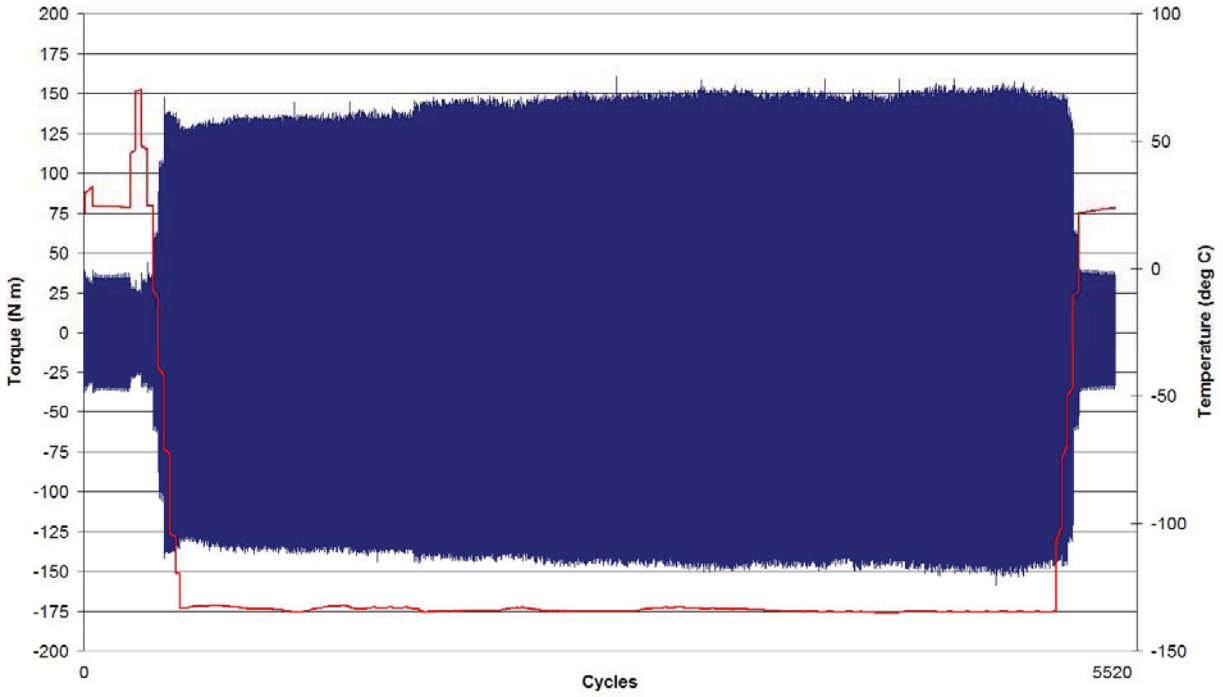

Figure 9: Friction Torque Plot
Polyamide-imide Bushings Greaseplated w/ Bray 601 vs. Anodized Aluminum

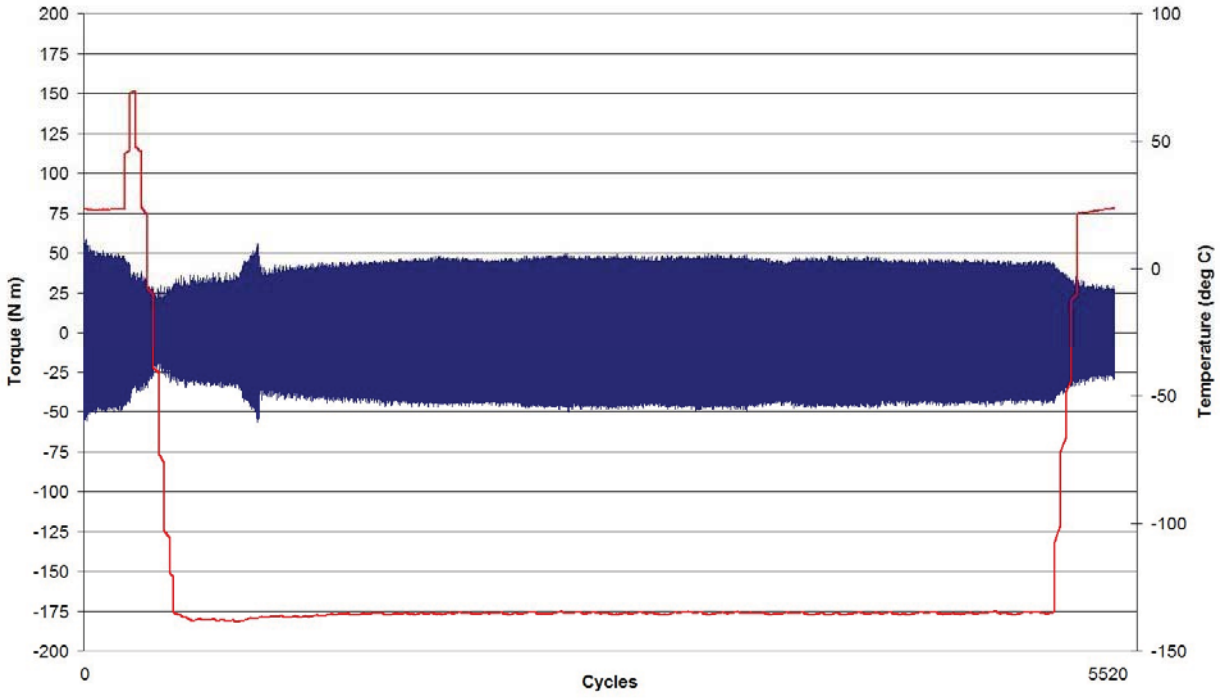

Figure 10: Friction Torque Plot
"Phosphate-like" Binder MoS_2 Bonded Film Coated Bushings vs. Titanium

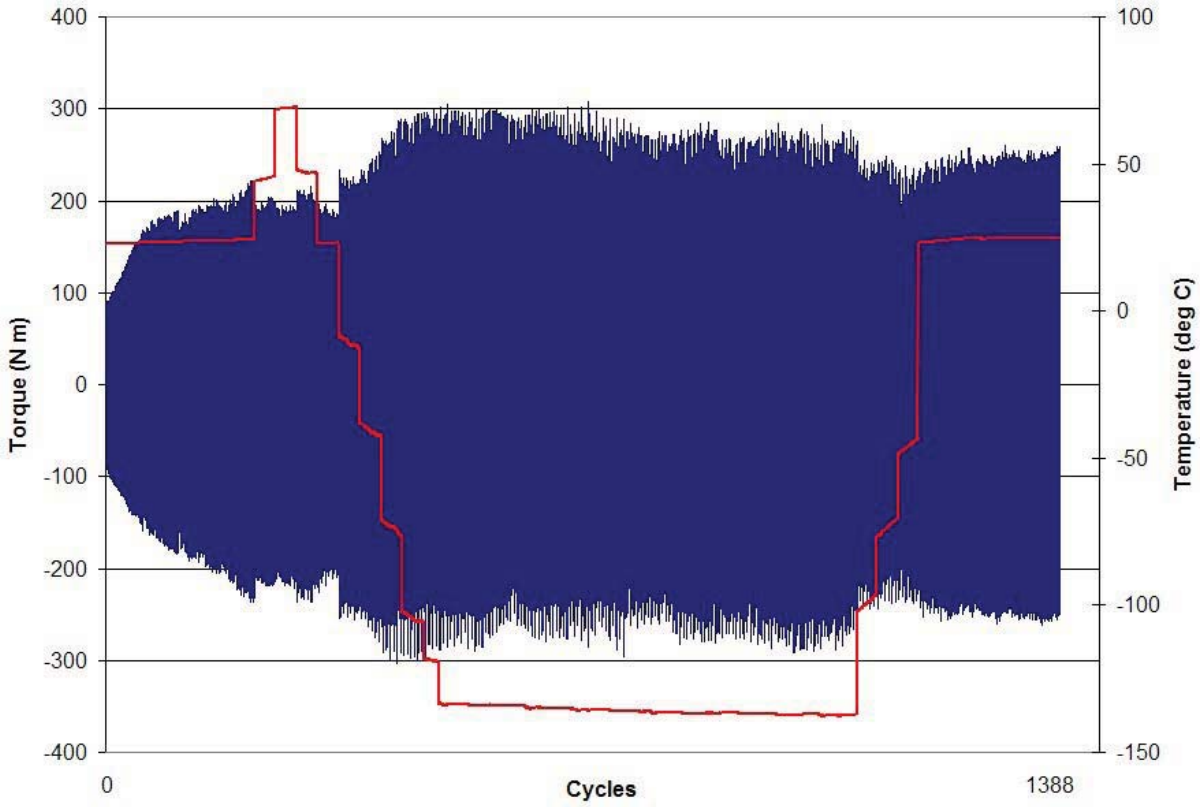

Figure 11: Friction Torque Plot
Bare Stainless Steel Bushings vs. Aluminum

Figure 12 illustrates the maximum (absolute value) friction torque, minimum (absolute value) peak friction torque, minimum peak torque at -135°C, and the difference between the maximum friction torque and minimum peak torque for each bushing test.

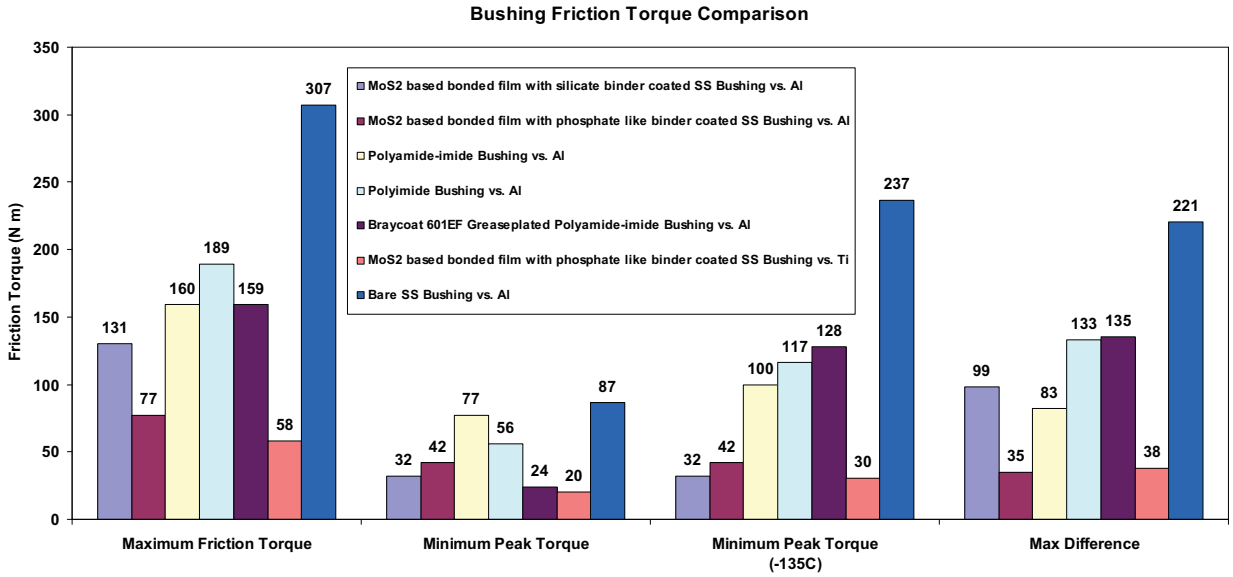

Figure 12: Bushing Friction Torque Comparison

One striking result of the bushing test series was the wide variation of friction torque over the test temperature profile. This variation was somewhat surprising as the coefficient of friction values for both bonded films and polymerics are not considered to be highly sensitive to temperature variation. If the coefficient of friction values were stable over temperature another mechanism must have been responsible for the friction torque variation during the testing. One possibility is that the mismatched, CTE induced, variable gaps between the shaft, the bushings, and the housing changed the contact geometry enough over temperature to produce the torque variation.

Another possible cause for the wide friction torque variation over temperature would be a test setup related systematic error. The setup for this test series was complex and involved the interaction of several large elements over a significant temperature range. The turnbuckle adjustments made to maintain a constant load on the driveshaft may have inadvertently altered the desired loading on the bushings. Although this is a possibility, the adjustments would not explain all of the torque variation over temperature.

In addition to the torque variation over temperature one sample also encountered an unexplained torque anomaly during testing. About midway through the cold dwell during the silicate binder MoS_2-bonded film test a torque ripple event occurred. The friction torque climbed steadily for several hundred cycles until peaking then abruptly self-correcting. It is difficult to definitively state what the cause of this event was given that the samples were not accessible at the time. That being said it was clear after disassembly of the pivot that a large amount of wear debris was generated during this test. The large volume of wear debris in the pivot could have shifted during the test and partially restricted the motion of one of the bushings. After some period of time the wear debris blockage could have cleared returning the assembly to a pre-event state. It is unknown whether this was an isolated event during just this test or this would be a repeatable behavior. The limited number of samples tested during this series does not provide any statically significant data to assess the repeatability of the behavior. None of the other samples exhibited this behavior during testing.

A review of the summary chart in Figure 12 illustrates the wide maximum friction torque variation between different bushing systems. The best performing bushing system with respect to maximum friction torque and maximum torque difference appears to be the “phosphate-like” binder MoS_2-based bonded film

coated stainless steel samples. The other MoS_2-based bonded film coated sample also exhibited good overall friction torque behavior compared to the polymeric samples.

An additional test was added during the test series to assess whether adding wet lubrication to the polyamide-imide bushings would improve the friction torque performance of that system throughout the operational temperature range. A set of polyamide-imide bushings was greaseplated with Braycote 601 and assembled in a test pivot to get hard data on the impact of adding the wet lube to the system. The results indicated there was a distinct benefit above -50°C but at lower temperatures the increased viscosity of the lubricant negatively impacted the performance of the bushing system by increasing the friction torque (compared to the unlubricated polyamide-imide samples).

Minimizing friction torque in the flight mobility pivots over temperature was desired to ensure the rover's suspension system articulates properly while traversing obstacles. Excessive drag in the pivots could significantly impair the mobile performance of the vehicle. This concern led the team to closely consider measured friction torque behavior in the selection of the final flight bushing material.

Wear

Relative bushing wear performance was also assessed as part of this test series. The nested configuration of the pivot assembly bushings prevented incremental wear monitoring during testing but thorough inspections were possible after each test.

Establishing a valid wear metric to quantify pivot assembly component wear has proven to be difficult. Some researchers have based wear rates on the volume of material lost during testing but this type of wear scar measurement was thought to be too complex for this application. With this in mind an alternative wear assessment approach was adopted involving photography of wear scars, profilimetry, and SEM microscopy.

JPL contracted with the Aerospace Corporation to analyze the worn bushing test samples [4,5]. The Aerospace Team photographed, provided SEM microscopy images, and performed profilimetry on the samples. A subset of the post test sample photographs taken by the team are shown in Figures 13 & 14. The overall wear performance of the samples was mixed with the bonded film coated samples exhibiting isolated but significant wear and the polymeric samples showing relatively light overall wear.

The MoS_2-based bonded film samples with the silicate binder performed most poorly with respect to wear generating large quantities of wear debris and significant wear scars on the outboard bushing. These wear scars were troubling as the lubricant film was completely worn away leaving metal to metal contact between the corner of the bushing and the contacting parts. Metal transfer occurred in this region as stainless steel particles were detected in the contacting end plate during the Aerospace Corp. analysis of the test samples. Measurable wear of the closeout plate itself was also documented in the analysis.

The MoS_2-based bonded film samples with the "phosphate-like" binder faired better during testing. Significant wear was limited to a small band on the corner of the coated outboard bushing. Stainless steel was exposed in that region but produced minimal wear on mating end plate in contrast to the silicate binder MoS_2 bonded film results.

Wear of the polyamide-imide and polyimide samples was very light. The team found that wear analysis of the polymeric materials was somewhat challenging as they are not coated so manufacturing scars look similar to wear scars.

The results of the wear assessment were in marked contrast to the friction torque results where the bonded films outperformed the polymerics. This was a troubling development as the team had hoped to find one superior bushing system that had both good friction torque performance and superior wear behavior. In the end, the team adopted a compromise position selecting the best performer with respect to friction torque accepting the non-ideal wear performance associated with that bushing system (MoS_2-based bonded film with "phosphate-like" binder).

Silicate binder MoS_2 bonded film coated Stainless

Phosphate-like binder MoS_2 bonded film coated Stainless

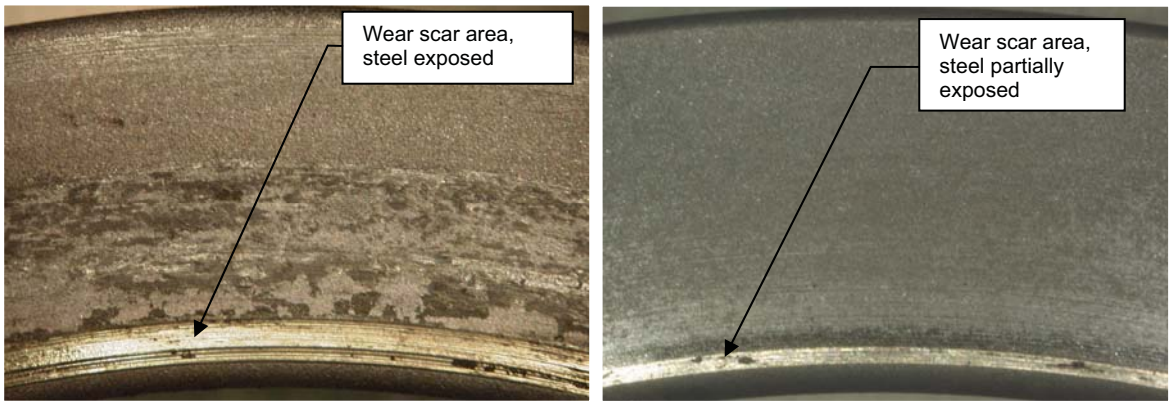

Figure 13: Post-Test Photos of Smaller, Outboard Bushing

Silicate binder MoS_2 bonded film Test

Phosphate-like binder MoS_2 bonded film Test

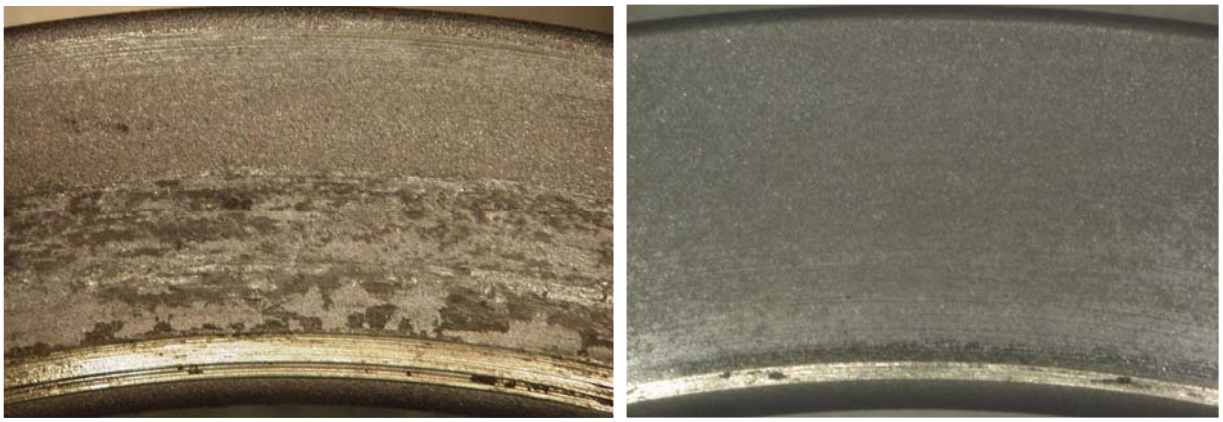

Polyamide-imide Test

Polyimide Test

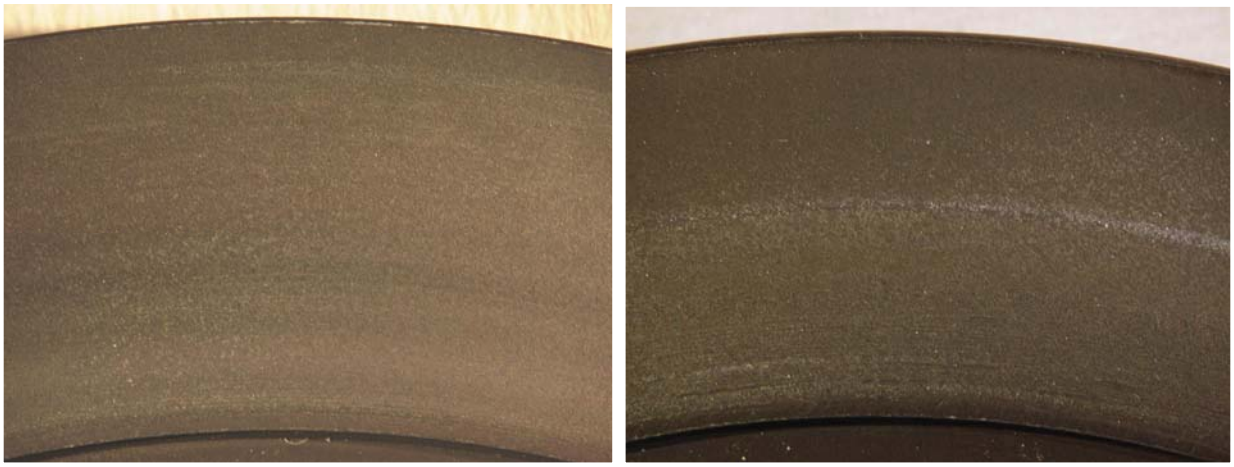

Figure 14: Post-Test Photos of Wear on Aluminum Pivot End Plates

Conclusion

The stated objectives of the bushing test series were to characterize the friction and wear performance of several candidate bushing/coating materials in a flight-like application and evaluate the behavior of these materials over the MSL operational temperature range. Both of these objectives were met during the testing and subsequent data analysis.

Although all test samples survived the modified 4x life test there were clear winners with respect to friction torque and wear. The MoS_2-based bonded film coated samples exhibited the best overall low friction behavior while the polyamide-imide samples had the least amount of wear among all bushing systems tested. Ultimately, the team selected the phosphate-like binder MoS_2-based bonded film / stainless steel bushing system for flight usage as minimizing the friction torque in the pivots was deemed more important than minimizing pivot wear during the mission.

The bushing test series has provided valuable friction and wear data on a variety of candidate bushing materials and lubricants enabling the MSL Mobility Team to make critical design decisions about flight pivots on the vehicle. This data should also prove valuable for future Mars Surface Systems considering the use of bushings in highly loaded pivots.

Acknowledgements

The research described in this paper was carried out at the Jet Propulsion Laboratory, California Institute of Technology, under a contract with the National Aeronautics and Space Administration.

The author would like to thank the following individuals and their respective teams for their contributions to this bushing test effort:

Donald Striebing, NASA Glenn Research Center:	Phase One Bushing Testing
Dr. Christopher DellaCorte, NASA Glenn Research Center:	Phase One Bushing Testing
Dr. Phillip Abel, NASA Glenn Research Center:	Phase One Bushing Testing
Ray Andres, Jet Propulsion Laboratory:	Test Fixture CAD Design Support
Dr. Jeffrey Lince, Aerospace Corp:	Sample Wear Analysis
Christopher Voorhees, Jet Propulsion Laboratory:	MSL Rover Mechanical Sys. Engineer
Jaime Waydo, Jet Propulsion Laboratory:	MSL Mobility Mechanical Team Lead

References

1. Striebing, Donald, “MSL Mobility Risk Reduction Bushing Test Series” (August 2006)
2. Waydo, Jaime "Dither Analysis Code." *Matlab Script*, (September 2005).
3. Young, W. *Roark’s Formulas for Stress and Strain 6th Ed*. Dallas, McGraw Hill, Inc., ©1989, p. 650.
4. Lince, Jeffrey, "SEM of MSL Lube Test Results", PowerPoint Presentation (November 2006)
5. Lince, Jeffrey, “SEM of MSL Lube Test Results”, PowerPoint Presentation (August 2006)